

A New Guidance Law for the Defense Missile of Nonmaneuverable Aircraft

Raghav Harini Venkatesan and Nandan Kumar Sinha

Abstract—In this brief, a new guidance law for the defense missile of nonmaneuverable aircraft is formulated based on dynamic game considerations. First, a simple differential game of protecting a static target in 2-D, involving simple motions for the attacker and defender, is introduced. The analysis is then extended to a moving noncooperative target in 2-D, in view of the fact that a nonmaneuverable aircraft would not be able to cooperate with the defender. A heuristic solution for the game is proposed and tested, and the results of the 2-D analysis are then extended to 3-D to formulate a new guidance law for the defense missile called the command to optimal interception point (COIP) guidance law. The validity of the new guidance law is checked using trajectory and envelope simulations, built with high-fidelity 6-DOF models using the computer-aided design of aerospace concepts in C++ framework. Performance comparisons are shown between the COIP guidance law and the recently proposed airborne command to line-of-sight (A-CLOS) guidance law. The results show that the performances of COIP and A-CLOS guidance laws are almost identical in a coplanar engagement scenario, but the COIP law has the additional advantage of working with only position information, without the knowledge of motion of the players. In addition, in a noncoplanar engagement case studied, the defense missile is shown to achieve intercept using the COIP guidance law, but fails when using the A-CLOS guidance law.

Index Terms—6-DOF simulations, computer-aided design of aerospace concepts in C++ (CADAC++), defense missile, differential game, guidance law, nonmaneuverable aircraft.

I. INTRODUCTION

PROTECTING an aircraft from an attacking missile using a defense missile is a much researched form of active aircraft defense. This is because traditional defense methods like flare or chaff countermeasures are rendered redundant by modern day sophisticated attacking missiles. Even if the attacking missile is susceptible to countermeasures, if it is launched from certain regions around the aircraft, countermeasures are ineffective [1]. This warrants the use of other methods to protect aircraft, such as a defense missile that would be launched from the target aircraft to intercept an attacking missile. Therefore, this three-body problem involving the aircraft, defense missile, and attacking missile, and deriving guidance laws for the defense missile has been of much interest in [2]–[4]. In [5]–[8], the guidance law for the defense missile was optimized when the attacker uses a specific guidance law like proportional navigation (PN).

Manuscript received September 28, 2014; revised January 22, 2015; accepted February 15, 2015. Date of publication April 27, 2015; date of current version October 12, 2015. Manuscript received in final form March 5, 2015. Recommended by Associate Editor Y. Ebihara.

The authors are with the Department of Aerospace Engineering, IIT Madras, Chennai 600036, India (e-mail: raghav.hv@gmail.com; nandan@ae.iitm.ac.in).

Color versions of one or more of the figures in this paper are available online at <http://ieeexplore.ieee.org>.

Digital Object Identifier 10.1109/TCST.2015.2411628

The airborne command to line-of-sight (A-CLOS) guidance law proposed in [8] manipulates two line-of-sight (LOS) rates associated with the three vehicles, and has benefits over the conventional three-point command to line-of-sight (CLOS) guidance law.

The objective of all the above studies essentially has been to derive optimal strategies for the target-defender team: pursuit laws for the defense missile and evasive maneuvers for the aircraft so as to avoid the attacking missile. In most real-life combat scenarios, the target aircrafts are fighters, and are therefore agile and able to cooperate with the defense missile by maneuvering. However, if the target aircrafts happen to be less maneuverable like airborne early warning and control (AEW&C) systems, they will be incapable of performing evasive maneuvers due to physical constraints. Therefore, the objective of this brief is to discuss the optimal strategy (guidance law) for the defense missile in the case of nonmaneuverable target aircraft.

II. METHODOLOGY

High-fidelity 6-DOF models for missiles and aircraft are used in this brief to perform simulations, as will be explained later in Section VI. Ideally, to derive the optimal guidance law for the defense missile, these high-fidelity models, with their full dynamics, must be taken into account while formulating the differential game (engagement scenario) between the attacking missile, defense missile, and the target aircraft. However, such a game problem formulated with complex dynamics is impossible to solve using currently known analytical and numerical methods. In addition, solutions to such differential games with complex dynamics could only be numerical, if possible at all.

Therefore, a simplified approach is taken in this brief, wherein the engagement scenario is modeled using simple motions for the attacker, defender, and target. The optimal strategy for the defender, found by solving the simplified differential game, is then directly applied to the high-fidelity simulations to study its applicability.

Following this approach, a simple differential game of protecting a static target in 2-D, involving simple motions for the attacker and defender, is introduced in Section III. The analysis is then extended to a moving noncooperative target in 2-D, in view of the fact that a nonmaneuverable aircraft like AEW&C systems would not be able to cooperate with the defender. In Section IV, the results of 2-D analysis for a noncooperative moving target are extended to 3-D, as a real-world engagement between an attacking missile, aircraft, and a defense missile cannot be expected to be coplanar. The analysis in 3-D is then used to formulate the command to optimal interception point (COIP) guidance law for the

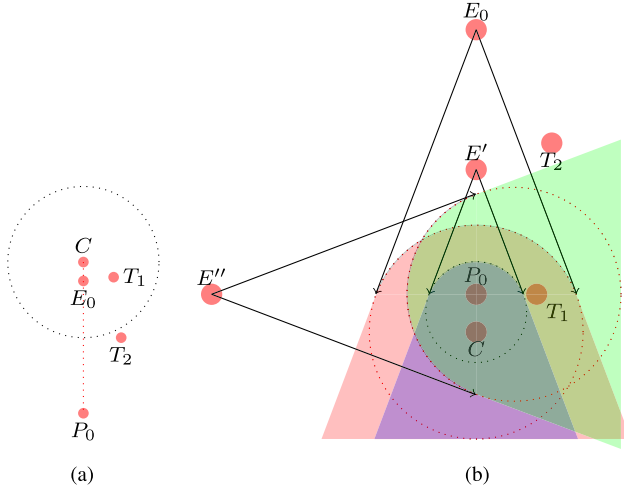


Fig. 1. Capture set and possible target locations T_1 and T_2 , within and outside the capture set, respectively [9]. (a) $v_p > v_e$. (b) $v_p < v_e$. Range of locations E can reach depending on position and orientation with respect to P .

defense missile in Section V. In Section VI, the validity of the formulated COIP guidance law is checked using trajectory and envelope simulations, and performance comparisons are shown between the COIP guidance law and the recently proposed A-CLOS guidance law [8]. In Section VII, the important conclusion from this brief is drawn.

III. GAME OF GUARDING A POINT TARGET IN 2-D

A. Static Target

In [9], the target-guarding game, which involves guarding a static point target T from an attacker (evader) E , by a defender (pursuer) P , was considered for P and E having simple motions with different speeds, such that $v_p : v_e :: p : e$, where v_p is the velocity of P and v_e is the velocity of E . The objective function of the game is the end time t_f , which corresponds to the capture of the target T by E — P strives to maximize it, whereas E strives to minimize it. The capture set in such a case happens to be an Apollonian circle (unlike a straight line when $v_p = v_e$), as shown in Fig. 1, with the center $C(x_c, y_c)$ and the radius R given by

$$C(x_c, y_c) = \left(\frac{x_{e0}p^2 - x_{p0}e^2}{p^2 - e^2}, \frac{y_{e0}p^2 - y_{p0}e^2}{p^2 - e^2} \right) \quad (1)$$

$$R = \sqrt{x_c^2 + y_c^2 - \frac{p^2(x_{e0}^2 + y_{e0}^2) - e^2(x_{p0}^2 + y_{p0}^2)}{p^2 - e^2}} \quad (2)$$

where $P_0(x_{p0}, y_{p0})$ and $E_0(x_{e0}, y_{e0})$ are the initial positions of the defender and attacker, respectively. It encloses E_0 if $v_p > v_e$, and P_0 if $v_p < v_e$, and its center C lies in line with P_0E_0 . It was shown that when $v_p < v_e$ [Fig. 1(b)], E can always capture T . This is because if P and E move closer toward each other when $v_p < v_e$, the size of the capture set would decrease, as shown in Fig. 1(b). This means that the regions that appeared inaccessible to E are now accessible because the size of the capture set is smaller. Therefore, E will always be able to reach any location on the plane, including that of T , by navigating sufficiently closer to P and detouring.

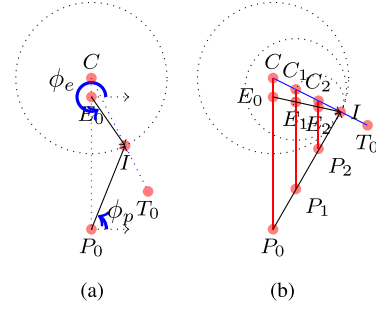


Fig. 2. Optimal strategies for P and E , for a static point target at T_0 ($v_p > v_e$) [9]. (a) Game geometry. (b) Game dynamics.

Therefore, T can be guarded only if $v_p > v_e$, and he is in P 's region, e.g., T_2 in Fig. 1(a), and not T_1 [9]. By shifting the origin of the coordinate system to (x_{p0}, y_{p0}) , and placing the y -axis along P_0E_0 , simpler expressions for (1) and (2) can be obtained. In the modified coordinate system

$$(x_{p0}, y_{p0}) = (0, 0) \quad (3)$$

$$(x_{e0}, y_{e0}) = (0, y'_{e0}) \quad (4)$$

$$(x_c, y_c) = \left(0, \frac{y'_{e0}}{1 - \frac{e^2}{p^2}} \right) \quad (5)$$

$$R = \frac{e}{p} \frac{y'_{e0}}{1 - \frac{e^2}{p^2}}. \quad (6)$$

Assuming $v_p > v_e$, the optimal strategy for each player was shown as heading to the optimal interception point (OIP) $I(x_i, y_i)$, which is the intersection of the line segment CT_0 (the line joining C and T 's static location T_0) with the capture circle, as shown in Fig. 2(a). The game ends with capture at I . An interesting observation presented was that although both P and E are continuously moving, I remains static if they both play optimally, as shown in Fig. 2(b). Therefore, in this case, the defender's and attacker's directions of heading (controls) ϕ_p and ϕ_e , shown in Fig. 2(a), are constant throughout the game, and both P and E traverse straight lines.

B. Moving Noncooperative Target

In the last section, optimal strategies for P and E were presented for a static T . This section deals with optimal strategies for P and E when T moves on his own free will, without any cooperation with P . The reason for this is twofold. First, the cooperative play between P and T against E has already been much researched in [2], [3], and [5]–[7]. Second, a nonmaneuverable aircraft like AEW&C cannot cooperate with its defense missile by tactical maneuvering. In view of these reasons, a noncooperative moving target is considered henceforth in this brief.

When T moves on his own free will, information about T 's movement will not be known to P and E *a priori*, as is the information about P and E 's movement to each other. It is assumed that the only information available to them would be their states and T 's state, i.e., the instantaneous locations $P(x_p, y_p)$, $E(x_e, y_e)$, and $T(x_t, y_t)$ in the case of simple motions.

In such a scenario, the optimal decisions of P and E would depend completely on their instantaneous locations and that of T . Therefore, if various snapshots of the game as it progresses are taken, the optimal strategies for P and E would depend on their locations and T 's location at each snapshot. In other words, the optimal strategies of P and E could be found by applying the results of the previous section at each such snapshot: head to the point $I(x_i, y_i)$, now calculated for the instantaneous locations $P(x_p, y_p)$, $E(x_e, y_e)$, and $T(x_t, y_t)$. Therefore, the point I too moves now with the movement of T , unlike Fig. 2(b). The control laws for P and E in this case now would be

$$\phi_p = \text{atan2}(y_i - y_p, x_i - x_p) \quad (7)$$

$$\phi_e = \text{atan2}(y_i - y_e, x_i - x_e) \quad (8)$$

where

$$(x_i, y_i) = \{(x_{i+}, y_{i+}) \text{ OR } (x_{i-}, y_{i-})\} \quad (9)$$

whichever is closest to $T(x_t, y_t)$, with

$$x_{i+} = \frac{x_c - mk + R\sqrt{1+m^2}}{1+m^2} \quad (10)$$

$$y_{i+} = m(x_{i+} - x_t) + y_t \quad (11)$$

$$x_{i-} = \frac{x_c - mk - R\sqrt{1+m^2}}{1+m^2} \quad (12)$$

$$y_{i-} = m(x_{i-} - x_t) + y_t \quad (13)$$

and

$$(x_c, y_c) = \left(\frac{x_e p^2 - x_p e^2}{p^2 - e^2}, \frac{y_e p^2 - y_p e^2}{p^2 - e^2} \right) \quad (14)$$

$$R = \sqrt{x_c^2 + y_c^2 - \frac{p^2(x_e^2 + y_e^2) - e^2(x_p^2 + y_p^2)}{p^2 - e^2}} \quad (15)$$

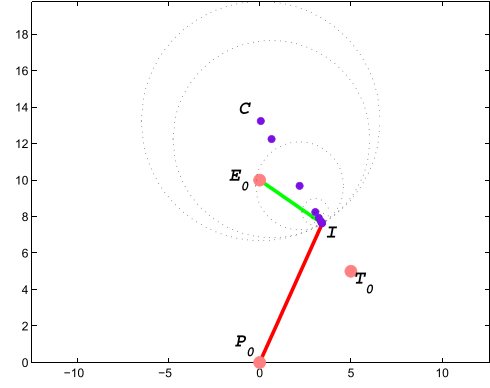
$$m = \frac{y_c - y_t}{x_c - x_t} \quad (16)$$

$$k = y_t - y_c - m x_t. \quad (17)$$

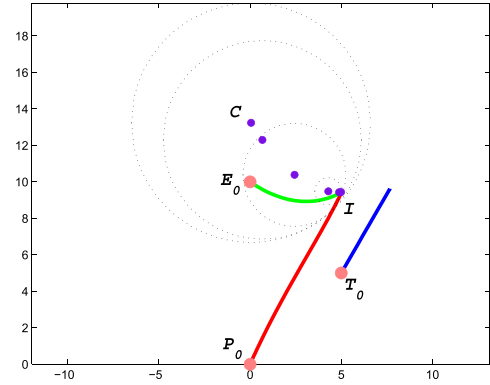
1) *Validation Tests:* The optimal paths of P and E when T moves freely, derived using (7) and (8), are tested for validity by performing simulations in MATLAB. The initial positions of P , E , and T are $P_0(0, 0)$, $E_0(0, 10)$, and $T_0(5, 5)$, respectively. The speeds of P and E are constant: $p = 2$ and $e = 1$.

a) *Both P and E play optimally:* Fig. 3(a) shows the optimal paths of P and E when T is static at T_0 . They traverse in straight lines toward I , which remains fixed and agrees with Fig. 2(b). It can be seen that the center of the instantaneous capture circle (denoted by the violet dots) moves along the line CT_0 , coalescing into I at capture. All the instantaneous capture circles touch each other at I .

Fig. 3(b) shows the optimal paths of P and E when T moves at an angle of 60° with respect to x -axis at a constant speed of $v_t = 1$, and his path is not known to P and E *a priori*. It can be seen that their optimal paths are now curved, as is the trajectory of C . The instantaneous circles no more touch each other at a single point, and the point I too keeps changing.



(a)



(b)

Fig. 3. Both P and E playing optimally. (a) T static. (b) T moving at 60° with respect to x -axis.

b) *P plays optimally, but E does not:* Fig. 4(a) shows the optimal path of P when E chooses to head straight down (which is different from his optimal path of heading toward I), for a static T at T_0 . It can be seen that this path turns out to be suboptimal for E , as P intercepts him further from T_0 than he did in Fig. 3(a). The instantaneous circles are starting to overlap, and their centers (shown by violet dots) traverse a curved path. P 's optimal path requires him to turn around to accommodate E 's suboptimal play, because his initial heading was based on expecting E to play optimally. At each instant, P chooses to head toward the instantaneous I , which is where E would head to if he resorted to optimal play at that instant. This is the best P could do, as the information of E 's path is not known to him *a priori*. If he knew, he would have headed straight up to intercept E at a much further point from T_0 .

Fig. 4(b) shows the optimal path of P when T moves at an angle of 60° with respect to x -axis at a constant speed of $v_t = 1$, with E choosing to head straight down like above. The path is worse for E than Fig. 4(a), as he did not accommodate for T 's movement in the other direction. However, the key difference from Fig. 4(a) is that P 's path is more curved because of the movement of T .

c) *E plays optimally, but P does not:* Fig. 5(a) shows a hypothetical case where P chooses to head along a

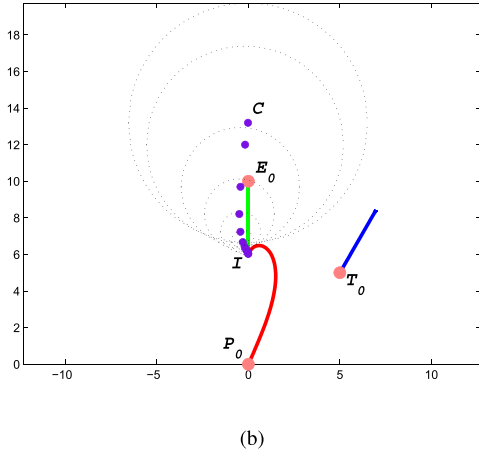
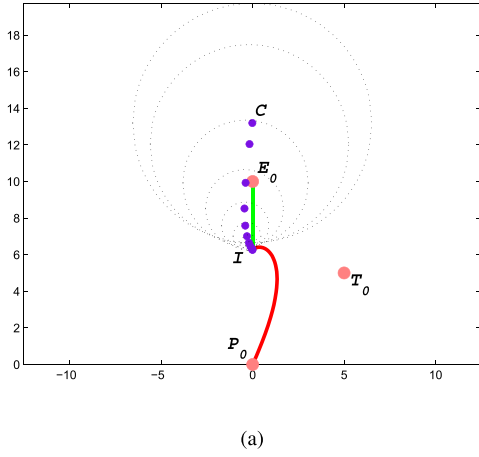


Fig. 4. P playing optimally, while E taking a suboptimal route. (a) T static. (b) T moving at 60° with respect to x -axis.

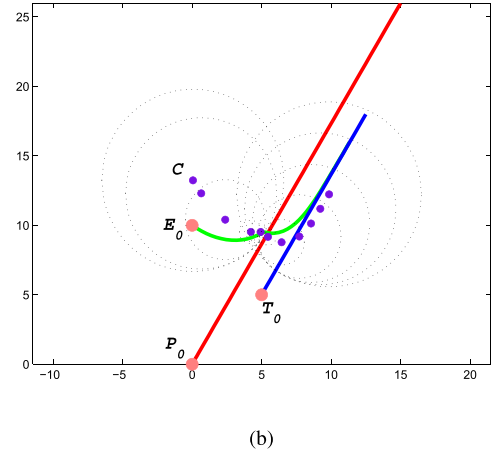
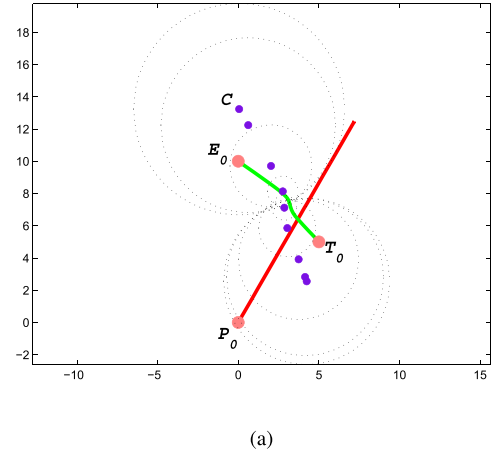


Fig. 5. P playing suboptimal, but E plays optimally. (a) T static. (b) T moving at 60° with respect to x -axis.

line making 60° with respect to x -axis while trying to guard a static T located at T_0 . However, E chooses to play optimally. It can be seen how E 's optimal strategy switches from navigating to I to T_0 itself. This happens as soon as the instantaneous capture circle starts enclosing T_0 , thus putting T_0 in a zone that E can reach before P . T is sacrificed in this case.

Fig. 5(b) repeats Fig. 5(a) with the difference that T too is now moving along a line making 60° with respect to x -axis with a constant speed of $v_t = 1$, starting from T_0 . Even in this case, P 's path is suboptimal, and he sacrifices T .

The simulations verify that the control laws of (7) and (8), formulated based on heuristic arguments, are indeed optimal for the players. This is because when P does not follow the control law of (7), his payoff in Fig. 5 is worse than that in Fig. 3. Similarly, when E does not follow the control law of (8), his payoff in Fig. 4 is worse than that in Fig. 3. It should be possible to verify their optimality in a more mathematically rigorous way too, following the analysis of life line game of pursuit [10], but a heuristic approach is taken in this brief as the focus is on their application, than the theory behind them.

IV. GAME OF GUARDING A POINT TARGET IN 3-D

A real active defense of an aircraft T by a defense missile P , from an attacking missile E , would take place in 3-D.

Therefore, it is necessary to extend the results of the previous section to 3-D, before they can be used to derive optimal guidance laws for the defense missile.

The key difference in 3-D is that, when the speeds of P and E are different, the capture set would be a sphere. The simplified expressions of (3)–(6) are helpful in understanding the capture sphere and optimal strategies with respect to the locations of P , E , and T .

Let O be the origin of the coordinate system describing the space in which the game is happening. Then

$$\vec{PE} = \vec{OE} - \vec{OP} \quad (18)$$

$$\vec{PT} = \vec{OT} - \vec{OP}. \quad (19)$$

From (3)–(5), it can be deduced that when E is a distance y'_{e0} away from P , C is a distance $y'_{e0}/(1 - (e^2/p^2))$ away from P along the same direction. Therefore, we can write

$$\vec{PC} = \frac{1}{1 - \frac{e^2}{p^2}} \vec{PE}. \quad (20)$$

In addition, from (6), it can be seen that the radius is (e/p) th of the distance between P and C . Therefore, we can write

$$R = \frac{e}{p} |\vec{PC}|. \quad (21)$$

From Fig. 2(a), it can be seen that the OIP I lies on the capture circle along the line C and T , which can be written as

$$\vec{CI} = R(\hat{CT}) = R \frac{\vec{CT}}{|\vec{CT}|}.$$

But

$$\begin{aligned} \vec{CT} &= \vec{PT} - \vec{PC} \\ \therefore \vec{CI} &= R \frac{\vec{PT} - \vec{PC}}{|\vec{PT} - \vec{PC}|}. \end{aligned}$$

The optimal heading direction of P is given by

$$\begin{aligned} \vec{PI} &= \vec{PC} + \vec{CI} \\ &= \vec{PC} + R \frac{\vec{PT} - \vec{PC}}{|\vec{PT} - \vec{PC}|} \\ &= \left(1 - \frac{R}{|\vec{PT} - \vec{PC}|}\right) \vec{PC} + \frac{R}{|\vec{PT} - \vec{PC}|} \vec{PT}. \quad (22) \end{aligned}$$

Vector equations (18)–(22) are very useful, as they are readily applicable in 3-D as well, whereas, (3)–(6) based on 2-D coordinates have to be reworked to be applicable in 3-D.

V. COMMAND TO OPTIMAL INTERCEPTION POINT GUIDANCE

One of the very popular guidance laws for missiles is that of PN. While this guidance law works well for an offensive missile pursuing a threat, it is not beneficial for a defense missile trying to protect an aircraft at beam-quarter aspects, i.e., aspects other than forward and rear quarters. Therefore, the focus henceforth in this brief will only be on the optimal strategy (guidance law) for the defense missile.

With the availability of (18)–(22), it is possible to formulate the optimal guidance law for the defense missile P . It is clear that the optimal guidance strategy of a defense missile at any instant should be to head toward I , which is the direction of the vector \vec{PI} given by (22).

The guidance law for P makes it pursue I by aligning its velocity vector \vec{V}_P with \vec{PI} , and can be written in terms of the normal (a_{ncom}) and lateral (a_{lcom}) acceleration commands to the missile

$$a_{ncom} = -\vec{a} \cdot \hat{P}_z \quad (23)$$

$$a_{lcom} = \vec{a} \cdot \hat{P}_y \quad (24)$$

with

$$\vec{a} = \frac{K}{|\vec{PI}|^4} (\vec{PI} \cdot \vec{V}_P) [(\vec{PI} \times \vec{V}_P) \times \vec{PI}] \quad (25)$$

where \hat{P}_z and \hat{P}_y are the unit vectors along the positive z -axis and y -axis of P 's body coordinate system, respectively, and K is the navigation gain. The guidance law of (23)–(25) is coined as the COIP guidance law, because the missile is commanded toward I at every instant of time. Thus, this law is a direct result of the optimal strategy for P derived in the previous sections. Although (25) points opposite to the direction of the required motion of P , the dot product (24) ensures the correct guidance command, because the sign convention used in aerospace computer-aided design

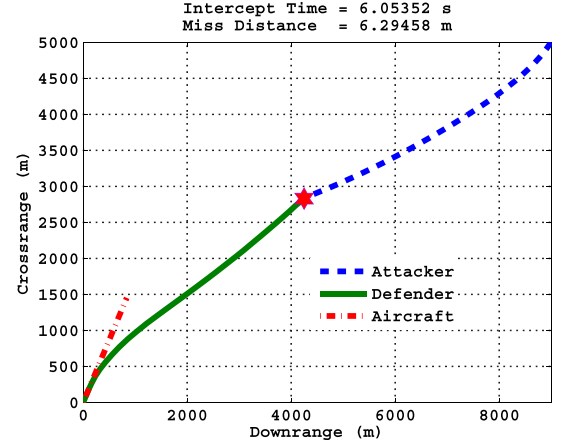


Fig. 6. Coplanar engagement—defense missile uses COIP guidance.

of aerospace concepts in C++ (CADAC++) simulations has the direction of the unit vector \hat{P}_y opposite to the conventional y -axis.

VI. VALIDATING THE COIP GUIDANCE LAW

In this section, the validity of the COIP guidance law is tested using simulations. For this, high-fidelity 6-DOF models are used. It is common to find that guidance algorithms are validated using simple kinematic or lower fidelity models. However, this was avoided for the study, because, in addition to representative simulations to prove the validity of the COIP guidance, as will be described later, missile envelopes too are generated to evaluate the efficiency of guidance algorithms when the attacking missile is detected at various ranges and aspects. Such envelopes would be reliable only if high-fidelity 6-DOF simulations are used.

The CADAC++ architecture is used to develop the models and simulations in this brief. It is a library of high-fidelity mathematical models in C++ for simulation of aerospace vehicles.

A. Trajectory Simulations

In this section, the COIP algorithm is validated using representative trajectory simulations. The aircraft is set to fly at an initial speed of 250 m/s. The navigation gain K of the missiles is 3, and the attacking missile always uses PN guidance. The defense missile is assumed to be launched in the heading direction of the aircraft. Both coplanar and noncoplanar engagements are studied.

Fig. 6 shows the trajectories of the vehicles for a coplanar engagement scenario, when the defense missile employs the COIP guidance law. It can be seen that the defense missile is successful in striking down the attacking missile. In addition, the intercept time and distance are marginally better than the case when the defense missile uses the recently proposed A-CLOS guidance law [8], shown in Fig. 7. The A-CLOS law provides some benefits over the well-known CLOS guidance law for defense missiles through some modifications. It can be seen that the trajectories of the defender in the two cases are hardly different.

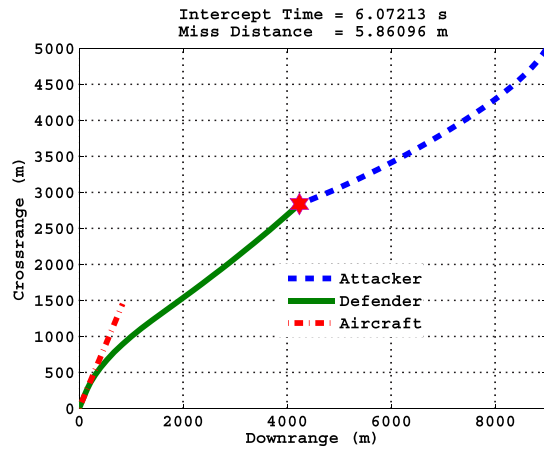


Fig. 7. Coplanar engagement—defense missile uses A-CLOS guidance.

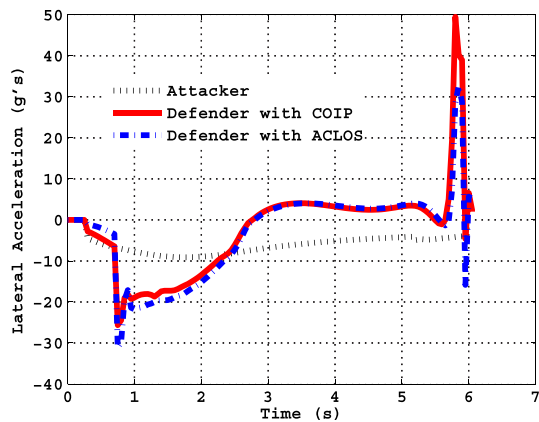


Fig. 8. Coplanar engagement—lateral acceleration profiles.

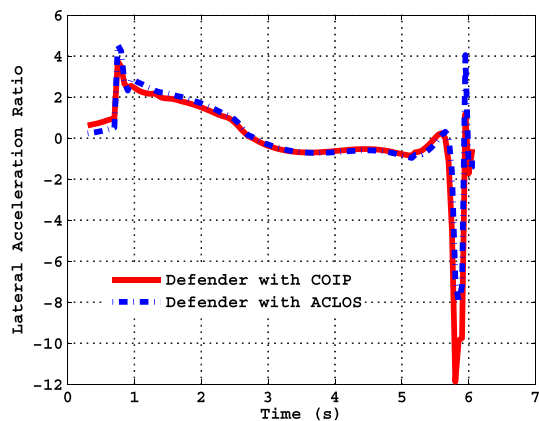


Fig. 9. Coplanar engagement—lateral acceleration ratios.

The lateral acceleration profiles for the defense missile while using COIP and A-CLOS guidance laws are compared in Fig. 8. Their corresponding ratios with the lateral acceleration of the aircraft are shown in Fig. 9. Figs. 8 and 9 show that compared with the A-CLOS guidance, the COIP guidance requires a higher negative *latax* (lateral acceleration) ratio (−12 versus −8), but a lower positive *latax* ratio (1 versus 4).

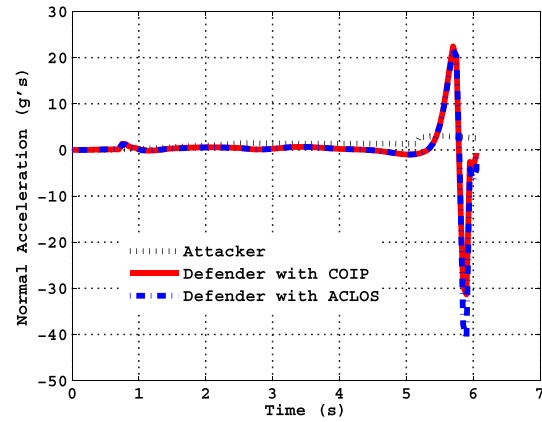


Fig. 10. Coplanar engagement—normal acceleration profiles.

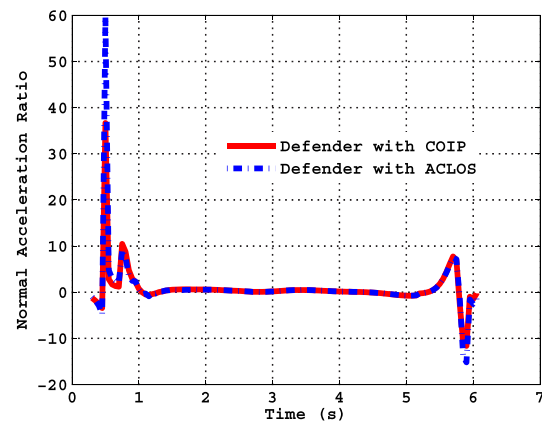


Fig. 11. Coplanar engagement—normal acceleration ratios.

The normal acceleration profiles for the defense missile while using COIP and A-CLOS guidance laws are compared in Fig. 10. There is not much difference between the two, except that the peak negative acceleration is −30 g for COIP guidance, while −40 g for A-CLOS guidance. However, the ratios of their accelerations with respect to the aircraft acceleration have a more pronounced difference, as shown in Fig. 11.

The provision to observe normal acceleration profiles is an advantage of using high-fidelity 6-DOF models for guidance studies. In kinematic simulations, when the engagement is assumed to be coplanar, the target aircraft moves in a plane. However, in reality, the aircraft's altitude will be fluctuating depending on the efficiency of its altitude hold autopilot. High-fidelity models capture this variation in altitude of the target aircraft. As a result, the normal accelerations of the missiles should not only compensate for gravity, but should also account for the target's altitude variation. As these normal acceleration commands are issued by the respective guidance laws of the missiles, their profiles look dissimilar for COIP and A-CLOS guidance laws, as shown in Fig. 10.

The trajectories of the vehicles for a noncoplanar engagement scenario, when the defense missile uses COIP guidance, are shown in Fig. 12. The aircraft is descending down in altitude, and therefore, the missiles are also losing altitude.

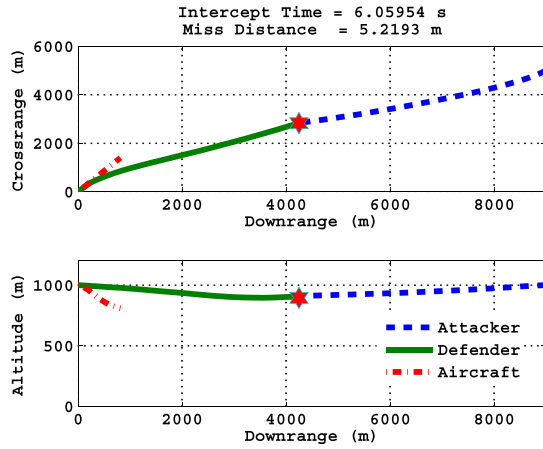


Fig. 12. Noncoplanar engagement—defense missile uses the COIP guidance.

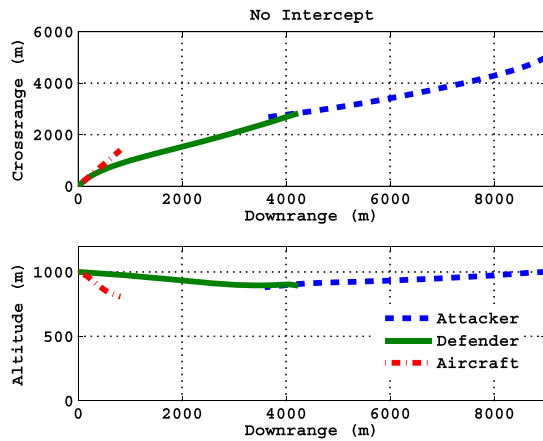


Fig. 13. Noncoplanar engagement—defense missile uses the A-CLOS guidance.

Even in this case, the defense missile intercepts the attacker. However, the intercept does not occur if the defense missile uses A-CLOS guidance, as shown in Fig. 13. The authors believe that this is one of the revelations of using 6-DOF simulations—the A-CLOS guidance law would have been predicted to achieve intercept using simple kinematic simulations, but with the use of high-fidelity simulations, its limitations are evident.

B. Envelope Studies

A defense missile used by an aircraft may not be able to intercept an attacking missile launched at all ranges and aspects around the aircraft. A few representative trajectory simulations like in the previous section, proving the validity of a guidance law for the defense missile cannot provide this information. A concise way of gathering this information is by studying missile envelopes. A missile envelope, for instance, like the one shown in Fig. 14, which corresponds to an unprotected nonmaneuvering aircraft, is the gray region, which marks locations around the aircraft from which missiles launched toward the aircraft would strike it down. The aircraft is assumed to be at the intersection of the cross hairs.

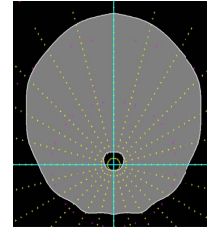


Fig. 14. Missile envelope for an unprotected nonmaneuvering aircraft.

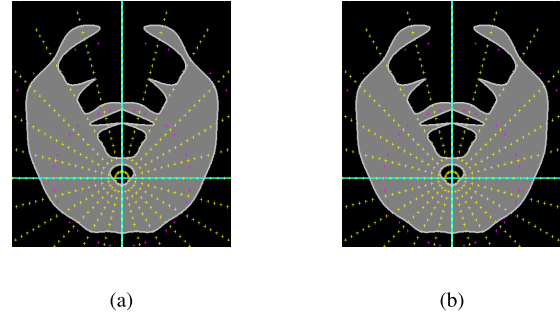


Fig. 15. Coplanar engagement missile envelope when the aircraft launches a defense missile directed along its heading direction. (a) Using COIP. (b) Using A-CLOS.

The interval between the yellow dots in Fig. 14 corresponds to a distance of 1 km, and each radial line is offset by 15° . The simulations are repeated till a maximum range of 25 km between the missile and aircraft. Therefore, a single envelope is the product of condensing the results of 575 simulations, although the number could be reduced to half, taking account of the symmetry for nonmaneuvering aircraft envelopes.

Having generated the unprotected missile envelope for a nonmaneuvering aircraft, the missile envelope for an aircraft deploying a defense missile is now generated using simulations. The initial heading of the defense missile is along the instantaneous velocity of the aircraft in these simulations. The resulting envelope when the defense missile uses COIP guidance law is shown in Fig. 15(a) and when it uses A-CLOS guidance law is shown in Fig. 15(b). It can be seen that the envelopes are almost identical. The reason why even a head-on course is not resulting in an intercept in Fig. 15 is because it was found that the defense missile was either not able to meet the minimum load factor requirement, or the required gimbals tracking rate exceeded the maximum tracking rate limit [1]. Unearthing such hidden limitations is a specialty of high-fidelity simulations, which would not be possible with simple kinematic simulations.

In the hypothetical case of the defense missile being allowed to have a variable initial heading: pointing toward the attacking missile when launched, the envelopes look like Fig. 16(a) and (b) for the defense missile using the COIP guidance and A-CLOS guidance laws, respectively. Even here, the two envelopes look almost identical.

From Figs. 6, 7, 15, and 16, it appears that the COIP and A-CLOS guidance laws have almost identical performance results on the defense missile in the coplanar engagement case.

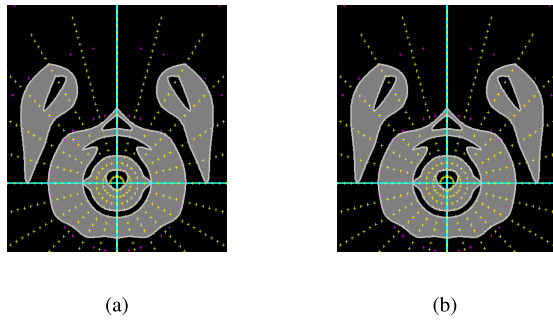


Fig. 16. Coplanar engagement missile envelope when the aircraft launches a defense missile directed toward the attacking missile. (a) Using COIP. (b) Using A-CLOS.

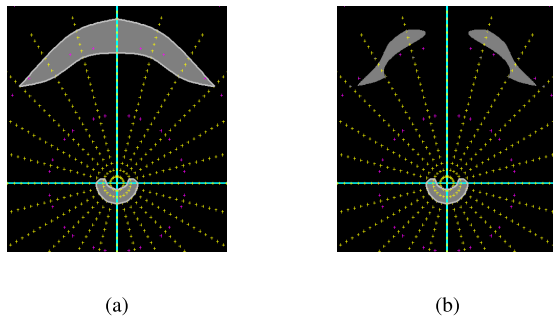


Fig. 17. Residual missile envelope. (a) Using countermeasures only [1]. (b) Using countermeasures, and a defense missile with the COIP guidance.

However, the acceleration requirement is slightly in favor of COIP guidance law in Fig. 11.

One of the revelations of the envelopes of Figs. 15 and 16 is that the defense missile *cannot* protect the aircraft at all ranges and aspects of the attacking missile. This fact is not evident in a few trajectory simulations illustrating the effectiveness of certain guidance laws for defense missiles, as has been done in numerous studies in the literature.

In [1], it was shown that even if countermeasures are used in different ways against attacking missiles, there is always some residual envelope area, as shown in Fig. 17(a). However, it appears that if the envelopes of Fig. 15(a) [Fig. 16(a) is excluded as the case is hypothetical] are taken into consideration, the resulting residual missile envelope area further shrinks, as shown in Fig. 17(b). The small envelope area in the

rear aspect at a short range can be neglected, as an AEW&C aircraft is unlikely to fly to regions where such an attack would be possible.

The above results suggest that the use of countermeasures and defense missiles together would help protect aircraft better, as the two would complement each other.

VII. CONCLUSION

The COIP guidance law presented in this brief is an improvement to the recently proposed A-CLOS guidance law as it is also designed to handle noncoplanar engagements. From the high-fidelity simulations conducted in this brief, it is evident that a defense missile alone cannot ensure safety of an aircraft against threats from various ranges and aspects, and combining it with countermeasures would be a better strategy for the safety of nonmaneuverable aircraft like AEW&C systems.

REFERENCES

- [1] R. H. Venkatesan and N. K. Sinha, "Key factors that affect the performance of flares against a heat-seeking air-to-air missile," *J. Defense Model. Simul., Appl., Methodol., Technol.*, vol. 11, no. 4, pp. 387–401, 2014.
- [2] J. Shinar and G. Silberman, "A discrete dynamic game modelling anti-missile defense scenarios," *Dyn. Control*, vol. 5, no. 1, pp. 55–67, Jan. 1995.
- [3] A. Perelman, T. Shima, and I. Rusnak, "Cooperative differential games strategies for active aircraft protection from a homing missile," *J. Guid., Control, Dyn.*, vol. 34, no. 3, pp. 761–773, 2011.
- [4] I. Rusnak, H. Weiss, and G. Hexner, "Guidance laws in target-missile-defender scenario with an aggressive defender," in *Proc. 18th IFAC World Congr.*, vol. 18, 2011, pp. 9349–9354.
- [5] V. Shaferman and T. Shima, "Cooperative multiple-model adaptive guidance for an aircraft defending missile," *J. Guid., Control, Dyn.*, vol. 33, no. 6, pp. 1801–1813, 2010.
- [6] T. Shima, "Optimal cooperative pursuit and evasion strategies against a homing missile," *J. Guid., Control, Dyn.*, vol. 34, no. 2, pp. 414–425, 2011.
- [7] A. Ratnoo and T. Shima, "Line-of-sight interceptor guidance for defending an aircraft," *J. Guid., Control, Dyn.*, vol. 34, no. 2, pp. 522–532, 2011.
- [8] T. Yamasaki, S. N. Balakrishnan, and H. Takano, "Modified command to line-of-sight intercept guidance for aircraft defense," *J. Guid., Control, Dyn.*, vol. 36, no. 3, pp. 898–902, May 2013.
- [9] R. H. Venkatesan and N. K. Sinha, "The target guarding problem revisited: Some interesting revelations," in *Proc. 19th World IFAC Congr.*, Cape Town, South Africa, Aug. 2014, pp. 1556–1561.
- [10] L. Petrosian, *Differential Games of Pursuit*, vol. 2. Singapore: World Scientific, 1993.